Article

Discovery Medicine 2025; 37(202): 2589–2601
https://doi.org/10.24976/Discov.Med.202537202.217

Pachymic Acid Protects Against Doxorubicin-Induced Cardiotoxicity Through Multi-Pathway Modulation of Oxidative Stress, Inflammation, DNA Damage, and Apoptosis

Yanxi Shi[1,2], Daxin Wang[1,2,*]

[1]Medical College of Yangzhou University, 225009 Yangzhou, Jiangsu, China
[2]Department of Cardiology, Taizhou People's Hospital, 225300 Taizhou, Jiangsu, China
*Correspondence: Daxinwang2002@gmail.com (Daxin Wang)
Submitted: 7 July 2025 Revised: 22 August 2025 Accepted: 2 September 2025 Published: 20 November 2025

Background: Doxorubicin (DOX), although widely employed in cancer therapy, induces significant cardiotoxicity primarily via oxidative stress and DNA damage. Pachymic acid (PA), a natural triterpenoid with established antioxidative and anti-inflammatory properties, has not yet been fully investigated for its protective actions against DOX-induced injury. This study aimed to explore the cardioprotective role of PA in mitigating DOX-induced cardiotoxicity, focusing on oxidative stress, inflammatory responses, DNA damage, and apoptosis.

Methods: H9c2 cardiomyocytes were treated with various concentrations of DOX and PA, either individually or in combination. The experimental groups consisted of control, DOX alone, PA alone, and PA plus DOX. A range of assays (CCK-8, TUNEL, ELISA, comet assay, Western blot) were performed to evaluate cell viability, apoptosis, inflammatory cytokine production, oxidative stress, and DNA damage. *In vivo*, the cardioprotective potential of PA was further evaluated in a rat model using histopathological analysis and serum biomarker evaluation.

Results: *In vitro*, PA pretreatment significantly improved cell viability and inhibited apoptosis in DOX-exposed H9c2 cells ($p < 0.01$), as demonstrated by modulation of Bcl-2, cleaved-PARP, Bax, and cleaved-caspase-3 expression ($p < 0.01$). PA suppressed oxidative stress by reducing reactive oxygen species (ROS) and Malondialdehyde (MDA) levels while enhancing Superoxide dismutase (SOD) and Glutathione (GSH) activities ($p < 0.01$). Additionally, PA mitigated DNA damage and downregulated DNA damage response proteins (p-ATR, γH2AX, P53, and P21) ($p < 0.01$). Proinflammatory cytokines tumor necrosis factor α (TNF-α), interleukin (IL)-6, and IL-1β were significantly decreased following PA treatment ($p < 0.01$). *In vivo*, serum concentrations of lactate dehydrogenase (LDH), cardiac troponin I (cTnI), brain natriuretic peptide (BNP), and creatine kinase-MB (CK-MB) were markedly reduced, and myocardial histopathology revealed alleviated structural damage ($p < 0.01$). These protective effects were accompanied by decreased oxidative damage, inflammatory responses, and cardiomyocyte loss in cardiac tissue ($p < 0.01$).

Conclusion: PA attenuated DOX-induced cardiotoxicity through the inhibition of oxidative stress, inflammatory responses, DNA damage, and apoptosis, highlighting its potential as a novel cardioprotective agent.

Keywords: pachymic acid; oxidative stress; doxorubicin; cardiotoxicity; DNA damage; cardiomyocyte apoptosis

Introduction

Doxorubicin (DOX), a widely used anthracycline chemotherapeutic, exhibits potent antitumor activity across diverse malignancies and remains a cornerstone of cancer therapy [1–3]. However, its dose-dependent cardiotoxicity poses a major limitation to clinical application, with incidence rates reported to reach up to 48% in high-dose regimens [4,5]. The hallmark of DOX-induced cardiotoxicity includes cardiomyocyte apoptosis, necrosis, and eventual progression to heart failure [6,7]. Mechanistically, oxidative stress is considered a primary mediator, as DOX metabolism generates excessive reactive oxygen species (ROS), leading to lipid peroxidation, mitochondrial dysfunction, and activation of cell death-associated pathways [8,9]. Moreover, DOX exacerbates cardiac injury through DNA damage and activation of the DNA damage response [10], involving key signaling pathways such as Nrf2/Keap1, SIRT1/p66Shc, and inflammatory mediators such as nuclear factor-kappa B (NF-κB) and the NOD-like receptor family pyrin domain containing 3 (NLRP3) inflammasome [11].

Given the pivotal roles of oxidative stress, apoptosis, and inflammation in DOX-induced cardiotoxicity, identifying effective cardioprotective agents remains an urgent clinical need. Pachymic acid (PA), a lanostane-type triterpenoid derived from *Poria cocos*, has attracted considerable interest due to its antioxidant, anti-inflammatory, and

antitumor activities [12–16]. Previous investigations have demonstrated that PA exerts tissue-protective properties by regulating the NF-κB pathway and mitigating myocardial ischemia/reperfusion injury through AMP-activated protein kinase (AMPK) activation [17,18]. Despite these promising pharmacological properties, the role of PA in counteracting DOX-induced myocardial toxicity has not yet been elucidated. Current strategies for DOX cardiotoxicity remain limited to dexrazoxane and lifestyle modifications [19], which provide only partial protection and fail to address multiple pathological pathways simultaneously. Conversely, the multitarget potential of PA to concurrently mitigate oxidative stress, inflammation, apoptosis, and DNA damage suggests a paradigm shift beyond existing single-mechanism approaches.

In this study, we systematically examined the cardioprotective effects of PA against DOX-induced myocardial injury, employing both cultured H9c2 cardiomyocytes (*in vitro*) and rat models (*in vivo*). These findings offer novel insights into the therapeutic potential of PA as a natural cardioprotective agent, with implications for improving the safety of DOX-based chemotherapy.

Materials and Methods

Reagents and Chemicals

Pachymic acid (PA, purity $\geq$98%; Fig. 1A) was obtained from Sigma-Aldrich (#PHL80512, St. Louis, MO, USA) and dissolved in DMSO (purity $\geq$99.9%, Sigma-Aldrich, St. Louis, MO, USA) to prepare stock solutions. DOX was purchased from MedChemExpress (#HY-15142A, USA). CCK-8 kit (#C0038) and TUNEL kit (#C1086) were sourced from Beyotime Biotechnology (Shanghai, China). A PCR-based mycoplasma detection kit (Myco-P-20, MycoAlert™, Lonza, Switzerland) was used to confirm cell culture quality. All reagents employed were of analytical grade.

Cell Maintenance and Drug Treatment

H9c2 rat cardiomyoblasts (ATCC® CRL-1446™) were obtained from the American Type Culture Collection and maintained in high-glucose DMEM (11965092, Gibco, Grand Island, NY, USA) supplemented with 10% FBS (A5670201, Gibco, Gibco, Grand Island, NY, USA) and 1% penicillin-streptomycin (Gibco) at 37 °C under 5% CO_2. Mycoplasma contamination was confirmed prior to experimentation using a PCR-based detection kit following the manufacturer's instructions, and all results were negative. The identity of H9c2 cells was verified based on their characteristic expression profile reported in the literature, including positive staining for desmin and α-sarcomeric actin and absence of endothelial (CD31) and hematopoietic (CD45) markers [20,21]. H9c2 cardiomyoblasts were selected as an established *in vitro* model for DOX cardiotoxicity due to their conserved cardiac-specific markers and reproducible sensitivity to oxidative stress, despite lacking full adult cardiomyocyte maturity, consistent with previous mechanistic study [22].

Dose-response assays were initially conducted to determine the effective concentration ranges of DOX (0–5 µM) and PA (0–60 µg/mL) [18,23]. The maximum non-toxic concentration of PA that did not alter H9c2 viability and the DOX concentration that produced the greatest reduction in viability were selected for subsequent assays. Based on these findings, cells were assigned to the following groups: (1) Control group: untreated H9c2 cardiomyocytes; (2) DOX group: cells treated with 5 µM DOX for 24 hours; (3) PA group: cells treated with 40 µg/mL PA for 12 hours; (4) DOX + PA group: cells sequentially treated with PA (40 µg/mL, 12 hours) followed by DOX (5 µM, 24 hours).

Animal Model and Treatment

All animal procedures were approved by the Experimental Animal Ethics Committee of the Guangdong Medical Experimental Animal Center (approval number: D202507-22), affiliated with the Guangdong Health Commission. Male Sprague-Dawley (SD) rats (6–8 weeks old, 200–220 g) were used to investigate the cardioprotective role of PA against DOX-induced cardiotoxicity. Animals were housed under standard laboratory conditions (12-hour light/dark cycle, 22 $\pm$ 2 °C, 50–60% humidity) with food and water available *ad libitum*. For all procedures, anesthesia was induced with 2% isoflurane (R510-22, RWD Life Science, China) in oxygen (1 L/min). Following deep anesthesia, blood was collected by cardiac puncture and centrifuged (3000 $\times$g, 10 minutes, 4 °C) to obtain serum, which was stored at –80 °C. Heart tissues were rapidly excised, rinsed in PBS (10010023, Gibco, Grand Island, NY, USA), and divided into aliquots for histology (fixed in 4% paraformaldehyde) or molecular analysis (snap-frozen in liquid nitrogen). Euthanasia was performed by cervical dislocation under deep anesthesia, confirmed by the absence of pedal reflex.

Rats were randomly allocated into four groups (n = 9 each): (1) Control group: intraperitoneal (i.p.) injections of saline twice weekly for 4 weeks, followed by daily oral gavage of saline for an additional 4 weeks; (2) DOX group: i.p. injections of DOX (2 mg/kg) twice weekly for 4 weeks, yielding a cumulative dose of 16 mg/kg, followed by daily oral saline gavage for 4 weeks [24]; (3) PA group: i.p. injections of saline twice weekly for 4 weeks, followed by daily oral gavage of PA (10 mg/kg) for 4 weeks [25]; (4) PA + DOX group: i.p. injections of DOX (2 mg/kg) twice weekly for 4 weeks (cumulative dose 16 mg/kg), followed by daily oral PA gavage (10 mg/kg) beginning the day after the final DOX injection and continued for 4 weeks.

The acute DOX model was chosen to investigate early mechanisms of cardiotoxicity, such as oxidative stress and apoptosis. While the model induces robust acute injury, it

does not fully mimic chronic human cardiotoxicity. To address this limit, we complemented it with histopathology and serum biomarkers, consistent with previously validated approaches [26].

Randomization was performed using a computer-generated sequence, with cage numbers assigned by an independent investigator. All histological assessments and data analyses were performed by investigators blinded to treatment allocation.

The post-treatment PA administration strategy was designed to: (1) simulate clinical scenarios in which cardioprotective interventions are typically initiated after chemotherapy, (2) specifically evaluate the therapeutic rather than prophylactic potential of PA, and (3) minimize potential pharmacokinetic interference during the peak toxicity phase of DOX.

CCK-8 Assay

Cell viability was assessed using the CCK-8 assay. Following treatment, cells were seeded into 96-well plates (1×10^4 cells/well), and 10 µL of CCK-8 reagent was added to each well, followed by incubation for 4 hours at 37 °C. Absorbance was measured at 405 nm using a microplate reader (iMark™, Bio-Rad, USA), and cell viability was expressed relative to control values. All experiments were performed in triplicate.

TUNEL Assay

Apoptosis in cultured cells and myocardial tissue was assessed using the TUNEL Apoptosis Detection Kit following the manufacturer's instructions. Briefly, treated H9c2 cells or paraffin-embedded cardiac sections were fixed with 4% paraformaldehyde (30 minutes, room temperature), permeabilized with 0.1% Triton X-100 in PBS (10 minutes), and incubated with TUNEL reagent for 1 hour at 37 °C in a humidified dark chamber. Cell nuclei were counterstained with DAPI for 5 minutes. TUNEL-positive cells were visualized using fluorescence microscopy (iMark™, Olympus, Japan) and quantified with ImageJ software (Version 1.54f, National Institutes of Health, Bethesda, MD, USA). Three independent experiments were performed, and at least three random fields per sample were analyzed.

ELISA Assay

Cell culture supernatants and serum aliquots were collected and stored at –80 °C until analysis. Levels of inflammatory cytokines, including tumor necrosis factor α (TNF-α) (#CSB-E11987r), interleukin (IL)-1β (#CSB-E08055r-IS), and IL-6 (#CSB-E04640r), were determined using commercial ELISA kits (Huamei Bio, China). Samples were incubated in antibody-coated plates according to the manufacturer's instructions. Absorbance was measured at 450 nm with a microplate reader (iMark™, Bio-Rad, USA). Cytokine concentrations were calculated using standard curves. Each sample was tested in duplicate, and assays were repeated independently three times.

Detection of Oxidative Stress and Cardiac Injury Markers

Oxidative stress was evaluated by measuring intracellular ROS, Malondialdehyde (MDA) (#A003-1, Jiancheng Bioengineering Institute, China), Superoxide dismutase (SOD, #A001-3, Jiancheng Bioengineering Institute, China), and Glutathione (GSH) (#A006-2, Jiancheng Bioengineering Institute, China). ROS was detected using the fluorescent probe DCFH-DA (#S0033S, Beyotime Biotechnology, Shanghai, China). After incubation with DCFH-DA (10 µM, 30 minutes, 37 °C), the fluorescence intensity of treated cells and tissues was measured using a spectrofluorometer (Fluoroskan FL, Thermo Fisher Scientific, USA) at 485/530 nm (excitation/emission). SOD activity (A001-3), MDA levels (A003-1), and GSH concentrations (A006-2) were quantified with colorimetric assay kits (Xavier Corporation, China) following the manufacturer's instructions.

Cardiac injury markers, including lactate dehydrogenase (LDH, CSB-E11324r), cardiac troponin I (cTnI, CSB-E08594r), brain natriuretic peptide (BNP, CSB-E07972r), and creatine kinase-MB (CK-MB, CSB-E14403r), were quantified using commercial kits (Huamei Bio, China) following the manufacturer's instructions. Measurements were derived from standard curves generated in parallel. All assays were conducted in triplicate and validated in three independent experiments.

Comet Assay

DNA damage was analyzed using a Comet Assay Kit (C2041M, Beyotime, China) following the manufacturer's protocol. Treated cells were suspended in low-melting-point agarose and layered onto pre-coated microscope slides. After solidification, slides were immersed in lysis buffer at 4 °C for 1 hour to lyse cells and release DNA. Electrophoresis was performed under alkalized conditions (25 V, 300 mA, 20–30 minutes), enabling migration of fragmented DNA. Slides were then neutralized, stained with SYBR Green, and examined using a fluorescence microscope (BX53, Olympus, Japan). DNA damage was quantified by calculating tail DNA percentage and tail moment using Comet Assay Software Project (Version 1.2.3, CASP, Poland) and ImageJ software (Version 1.54f, National Institutes of Health, USA).

Western Blot

Whole-cell proteins were extracted from cells or myocardial tissues using RIPA buffer (P0013B, Beyotime Biotechnology, Shanghai, China) supplemented with protease and phosphatase inhibitors. Protein concentrations were determined by the BCA assay (23227, Thermo Fisher Scientific, Waltham, MA, USA), and equal amounts (30 µg) were separated on 10% SDS-PAGE gels before transfer to PVDF membranes (IPVH07850, Millipore, Billerica, MA, USA). After blocking with 5% non-fat milk for 2 hours

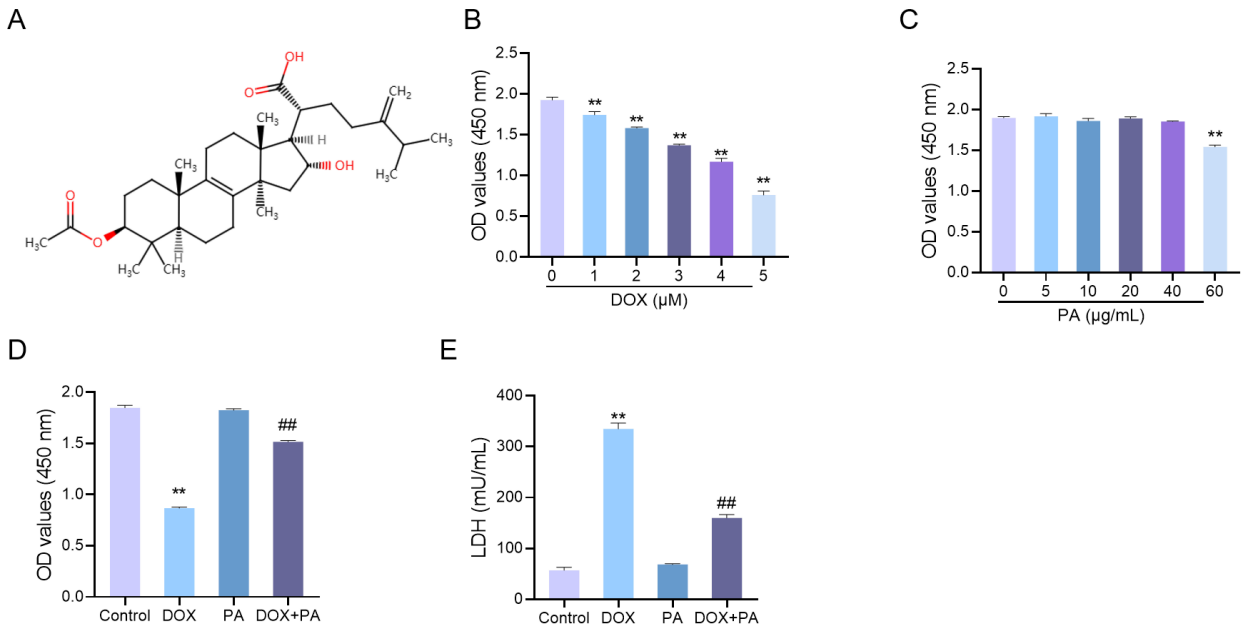

Fig. 1. Pachymic acid (PA) attenuates doxorubicin (DOX)-induced cytotoxicity and enhances H9c2 cell viability. (A) Chemical structure of PA. (B) H9c2 cell viability following exposure to varying concentrations of DOX (0–5 μM) assessed by CCK-8 assay. (C) Effects of PA (0–60 μg/mL) on H9c2 cell viability. (D) PA pretreatment alleviated DOX-induced decline in cell viability. (E) Lactate dehydrogenase (LDH) release was significantly increased by DOX and reduced by PA pretreatment. Data are presented as mean ± SD (n = 3 independent experiments for *in vitro* assays; n = 9 animals per group for *in vivo* studies). $^{**}p < 0.01$ vs. control; $^{\#\#}p < 0.01$ vs. DOX.

at room temperature, membranes were incubated overnight at 4 °C with primary antibodies: anti-Bcl-2 (ab182858), anti-cleaved-PARP (ab32064), anti-Bax (ab32503), anti-cleaved-caspase 3 (ab2302), anti-ATR (ab2905), anti-p-ATR (ab223258), anti-γH2AX (ab81299), anti-P53 (ab26), anti-P21 (ab109520), and anti-β-actin (ab8226) (all from Abcam). Antibody dilutions were as follows: anti-Bcl-2 (1:1000), anti-cleaved-PARP (1:2000), anti-Bax (1:1000), anti-cleaved-caspase 3 (1:1000), anti-ATR (1:800), anti-p-ATR (1:1000), anti-γH2AX (1:1000), anti-P53 (1:800), anti-P21 (1:1000), and anti-β-actin (1:2000). After washing, membranes were incubated with HRP-conjugated secondary antibodies (1:5000 dilution; goat anti-rabbit: ab205718; goat anti-mouse: ab205719) for 1 hour at room temperature. Protein bands were visualized using an ECL detection system (ChemiDoc™ MP, Bio-Rad, Hercules, CA, USA) and quantified with ImageJ software (Version 1.54f, National Institutes of Health, USA). Target protein expression was normalized to β-actin.

Histopathological Analysis

Heart tissues were fixed in 4% paraformaldehyde (P0099; Beyotime, China) for 24 hours, dehydrated in graded ethanol and embedded in paraffin. Sections (5 μm) were prepared, deparaffinized with xylene, and rehydrated in descending ethanol concentrations. Hematoxylin staining was performed for 5 minutes, followed by eosin staining for 2 minutes. Histopathological changes in myocardial architecture, including cellular arrangement, fibrosis, and inflammatory infiltration, were examined under light microscopy (CX43, Olympus, Japan).

Statistical Analysis

Data were analyzed using SPSS 23.0 (IBM, USA) and expressed as mean ± SD. *In vitro* experiments were independently repeated three times (n = 3). For *in vivo* studies, each group consisted of nine rats (n = 9). Group comparisons were performed by one-way ANOVA followed by Tukey's post hoc test. A p-value < 0.05 was considered statistically significant.

Results

PA Attenuates DOX-Induced Cytotoxicity and Improves H9c2 Cell Viability

To evaluate DOX-induced cytotoxicity and the protective potential of PA, a dose-response analysis was conducted using the CCK-8 assay in H9c2 cardiomyocytes. Cell viability progressively decreased with increasing DOX concentrations, reaching a minimum of approximately 40%

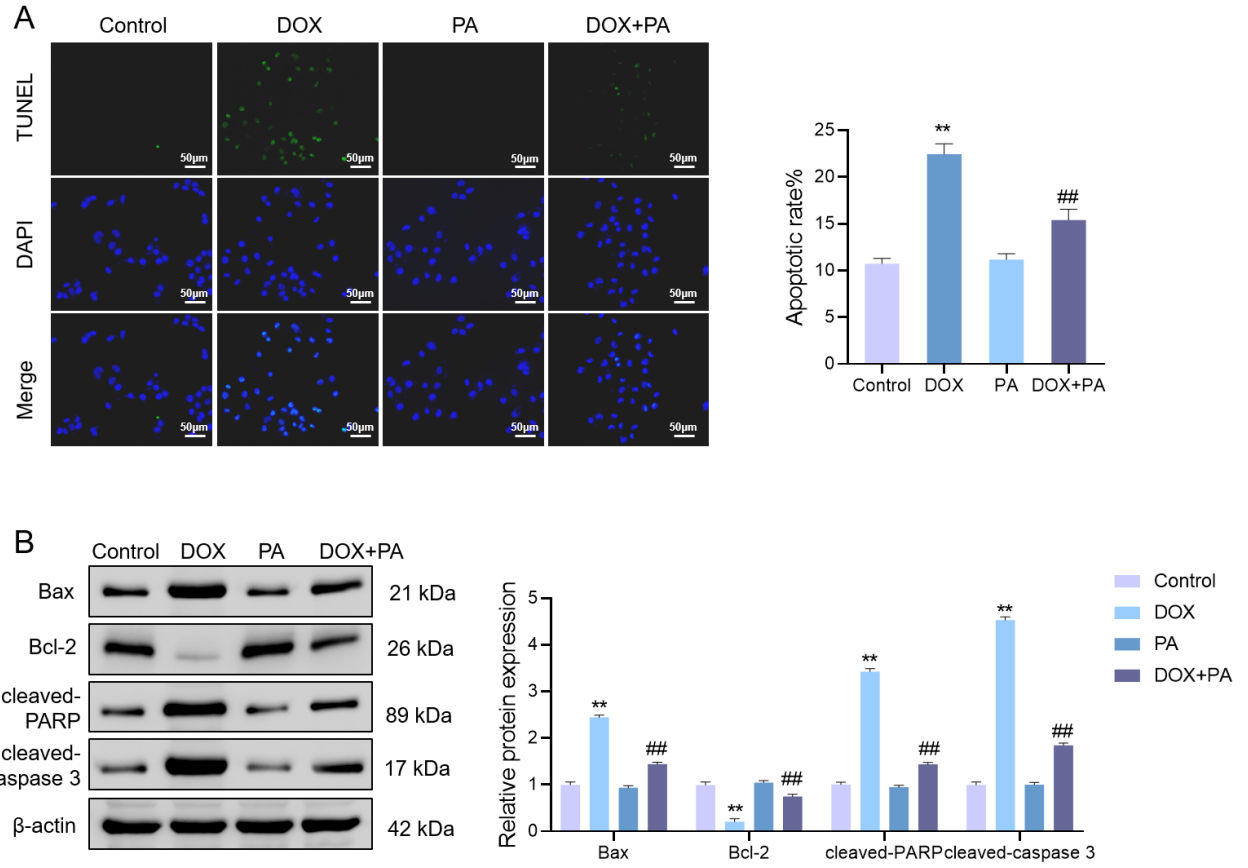

Fig. 2. PA reduces DOX-induced apoptosis in H9c2 cells. (A) TUNEL assay showing TUNEL-positive cells (green) and 4′, 6-diamidino-2-phenylindole (DAPI)-stained nuclei (blue). (B) Western blot analysis of Bax, Bcl-2, cleaved-PARP, and cleaved-caspase 3. Data are presented as mean ± SD (n = 3 independent experiments for *in vitro* assays; n = 9 animals per group for *in vivo* studies). $^{**}p < 0.01$ vs. control; $^{\#\#}p < 0.01$ vs. DOX.

at 5 μM (Fig. 1B). The cytotoxicity profile of PA was subsequently assessed. PA treatment at concentrations between 0–40 μg/mL had no significant effect on cell viability, whereas 60 μg/mL markedly reduced viability ($p < 0.01$), establishing 40 μg/mL as the maximal non-cytotoxic concentration for subsequent experiments (Fig. 1C).

To examine the protective effect of PA, H9c2 cells were pretreated with PA (40 μg/mL) prior to DOX exposure. As anticipated, PA pretreatment significantly ameliorated DOX-induced cytotoxicity, as evidenced by enhanced cell viability and reduced LDH release compared to DOX treatment alone ($p < 0.01$; Fig. 1D,E).

These results indicate that PA mitigates DOX-induced cytotoxic injury and preserves cardiomyocyte viability through its cytoprotective properties.

PA Inhibits DOX-Mediated Apoptosis in H9c2 Cardiomyocytes

The anti-apoptotic effect of PA was evaluated using TUNEL staining and Western blot analysis. As shown in Fig. 2A, DOX treatment markedly increased the proportion of TUNEL-positive cells relative to the control group ($p < 0.01$), confirming significant induction of apoptosis. PA alone exerted no significant effect on apoptosis, with TUNEL-positive cell numbers comparable to control. Notably, PA pretreatment markedly reduced the number of apoptotic cells in the DOX + PA group compared to DOX treatment alone ($p < 0.01$).

Western blot analysis further revealed that PA pretreatment attenuated DOX-induced alterations in apoptosis-related proteins, downregulating pro-apoptotic markers while restoring anti-apoptotic protein expression ($p < 0.01$; Fig. 2B). TUNEL assay results were consistent, confirming significantly reduced apoptosis in PA-treated cells ($p < 0.01$; Fig. 2A).

Collectively, these findings indicate that PA alleviates DOX-induced apoptosis in H9c2 cardiomyocytes.

PA Inhibits DOX-Induced Inflammatory Response in H9c2-Derived Cardiomyoblasts

The anti-inflammatory activity of PA was examined by quantifying TNF-α, IL-6, and IL-1β levels in H9c2 culture supernatants using ELISA. DOX treatment significantly elevated the release of inflammatory cytokines

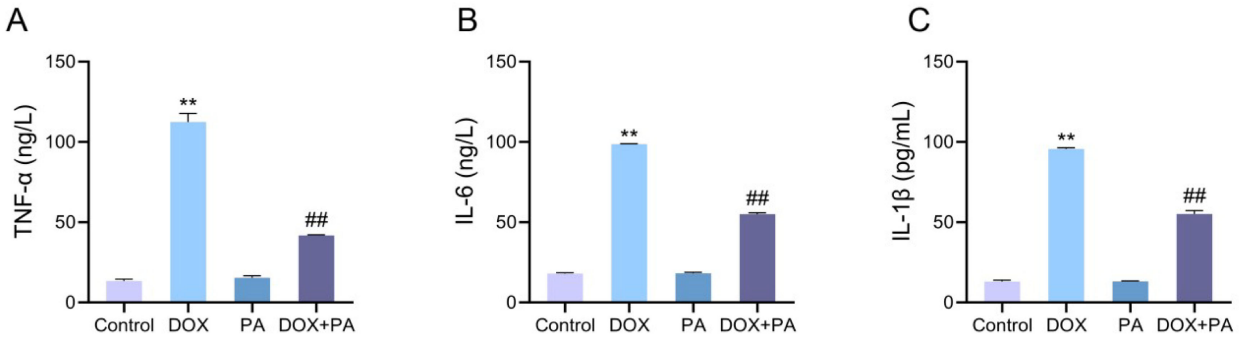

Fig. 3. PA suppresses DOX-induced inflammatory cytokine release in H9c2 cells. (A) Tumor necrosis factor α (TNF-α) production. (B) Interleukin (IL)-6 production. (C) IL-1β production. Data are presented as mean $\pm$ SD (n = 3 independent experiments for *in vitro* assays; n = 9 animals per group for *in vivo* studies). $^{**}p < 0.01$ vs. control; $^{\#\#}p < 0.01$ vs. DOX.

(TNF-α, IL-6, IL-1β; Fig. 3A–C), whereas PA co-treatment significantly reduced their levels ($p < 0.01$ vs. DOX). These findings demonstrate that PA effectively suppresses DOX-induced inflammatory responses in cardiomyocytes.

PA Mitigates DOX-Induced Oxidative Stress in H9c2 Cells

To investigate the oxidative stress-modulating properties of PA, oxidative burden markers were quantified in H9c2 cells following DOX treatment. PA treatment significantly attenuated DOX-induced oxidative stress by decreasing ROS and MDA levels while restoring SOD and GSH activities ($p < 0.01$; Fig. 4A–D). These findings suggest that PA effectively reduces DOX-induced oxidative stress.

PA Attenuates DOX-Mediated Genotoxic Stress in H9c2 Cardiomyocytes

DNA damage is a key mechanism of DOX-induced cardiotoxicity. Comet assay analysis (Fig. 5A) revealed that DOX significantly elevated genotoxicity in H9c2 cells, as indicated by elevated tail DNA % and tail moment compared to the control ($p < 0.01$). Co-treatment with PA markedly reduced DNA damage relative to DOX alone ($p < 0.01$).

To further validate these findings, DNA damage response proteins were examined by Western blot. PA pretreatment attenuated DOX-induced DNA damage, as evidenced by decreased expression of p-ATR, γH2AX, P53, and P21 ($p < 0.01$; Fig. 5B).

These findings demonstrate that PA significantly suppresses DOX-induced DNA damage and inhibits activation of the DNA damage response pathway.

PA Improves DOX-Induced Myocardial Dysfunction in Vivo

To evaluate the cardioprotective role of PA *in vivo*, functional indicators and serum cardiac injury markers were assessed in DOX-treated rats. PA treatment significantly alleviated DOX-induced cardiac dysfunction, as evidenced by preserved heart rate, reduced left ventricular diameters (left ventricular end-diastolic dimension (LVEDD) and left ventricular end-systolic dimension (LVESD)), and enhanced systolic function (increased ejection fraction (EF) and fractional shortening (FS)) compared to DOX-treated rats ($p < 0.01$; Fig. 6A–E). These echocardiographic findings confirm the protective effects of PA on both structural and functional cardiac parameters in DOX-induced cardiotoxicity. Serum biomarkers of cardiac injury (LDH, cTnI, BNP, CK-MB) were also markedly elevated by DOX but significantly reduced following PA treatment ($p < 0.01$; Fig. 6F–I). Collectively, these results suggest that PA mitigates DOX-induced myocardial dysfunction and tissue injury.

PA Mitigates DOX-Mediated Apoptosis and Myocardial Injury in Animal Models

The protective effects of PA on DOX-induced myocardial apoptosis were evaluated histologically and at the molecular level. Histopathological analysis demonstrated that PA alleviated DOX-induced myocardial damage, reducing fiber disruption, necrosis, and apoptotic cell death ($p < 0.01$; Fig. 7A,B). Western blot analysis (Fig. 7C) showed that DOX treatment upregulated Bax, cleaved-PARP, and cleaved-caspase 3, while downregulating the expression of Bcl-2 ($p < 0.01$). PA intervention significantly counteracted these changes, significantly decreasing Bax, cleaved-PARP, and cleaved-caspase 3 while restoring Bcl-2 expression ($p < 0.01$).

Collectively, these findings demonstrate that PA reduces myocardial apoptosis and damage by modulating apoptosis-related protein expression in DOX-treated rats.

PA Reduces Inflammation and Redox Imbalance Induced by DOX in Rats

To further explore the mechanisms underlying the cardioprotective role of PA, systemic inflammatory cytokines and oxidative indicators were measured in DOX-treated rats. PA treatment significantly suppressed proinflamma-

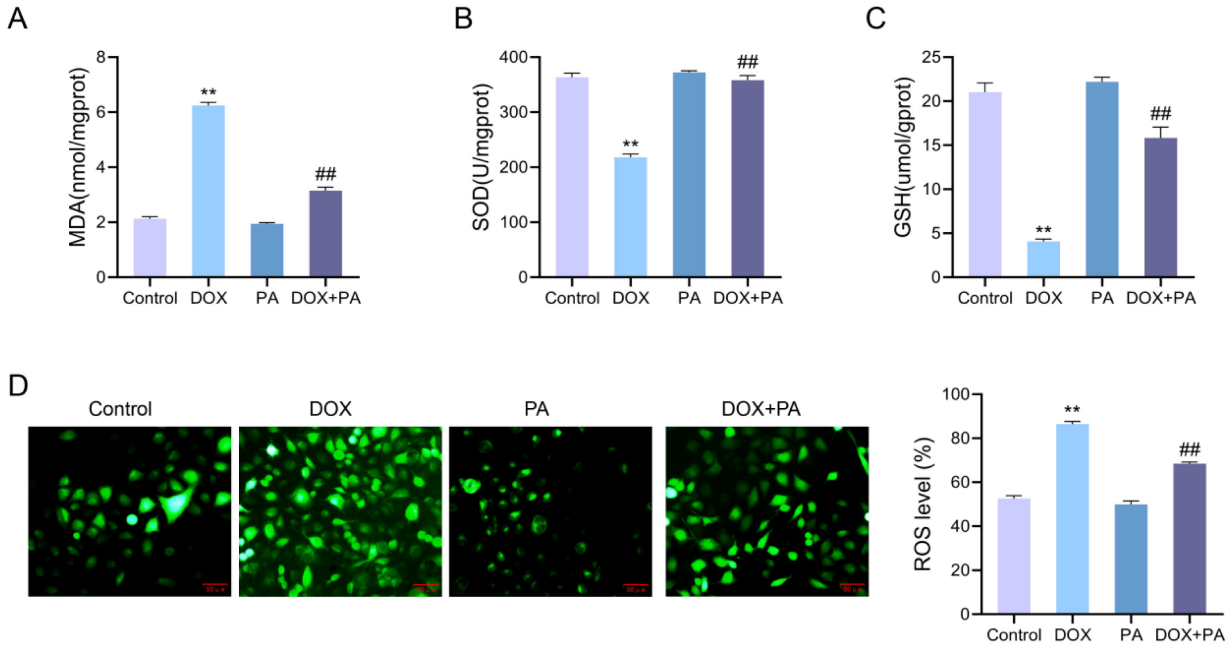

Fig. 4. PA mitigates DOX-induced oxidative stress in H9c2 cardiomyocytes. (A) Malondialdehyde (MDA) levels. (B) Superoxide dismutase (SOD) activity. (C) Glutathione (GSH) content. (D) Reactive oxygen species (ROS) levels. Data are presented as mean ± SD (n = 3 independent experiments for *in vitro* assays; n = 9 animals per group for *in vivo* studies). $^{**}p < 0.01$ vs. control; $^{\#\#}p < 0.01$ vs. DOX.

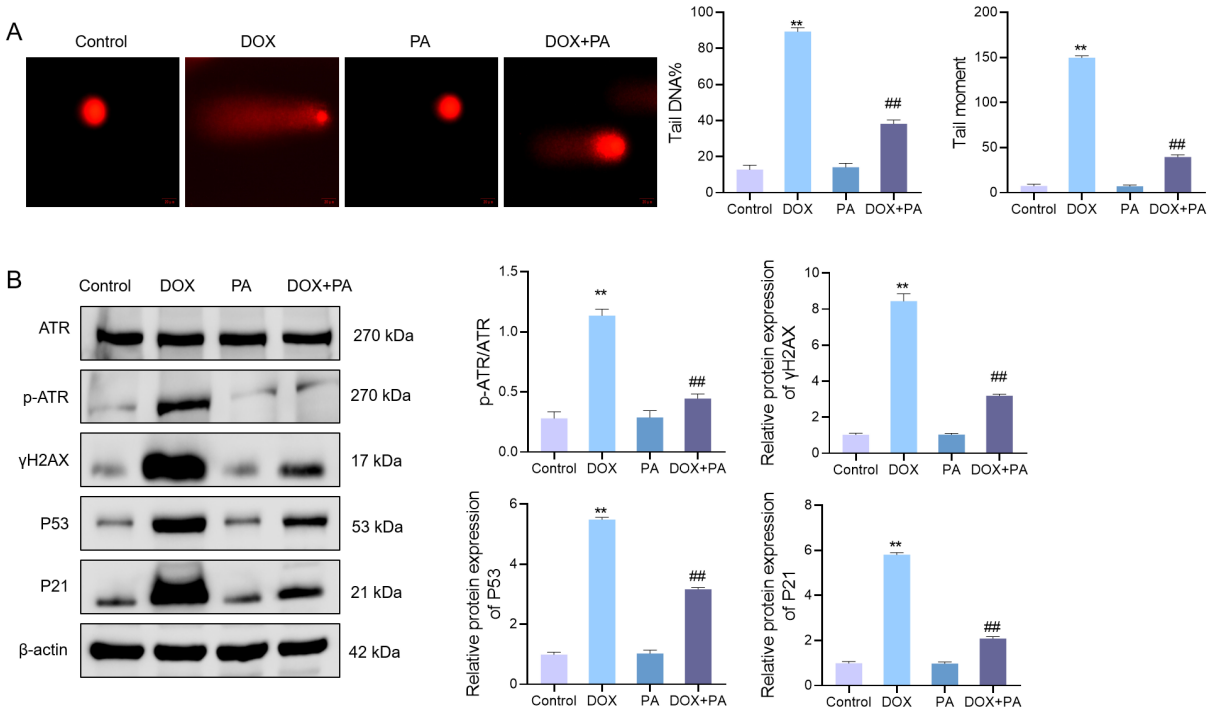

Fig. 5. PA alleviates DOX-induced DNA damage in H9c2 cells. (A) Representative comet assay images showing DNA damage (left) and quantitative analysis of tail DNA % and tail moment (right). (B) Western blot analysis of DNA damage response proteins ATR, p-ATR, γH2AX, P53, and P21. Data are presented as mean ± SD (n = 3 independent experiments for *in vitro* assays; n = 9 animals per group for *in vivo* studies). $^{**}p < 0.01$ vs. control; $^{\#\#}p < 0.01$ vs. DOX.

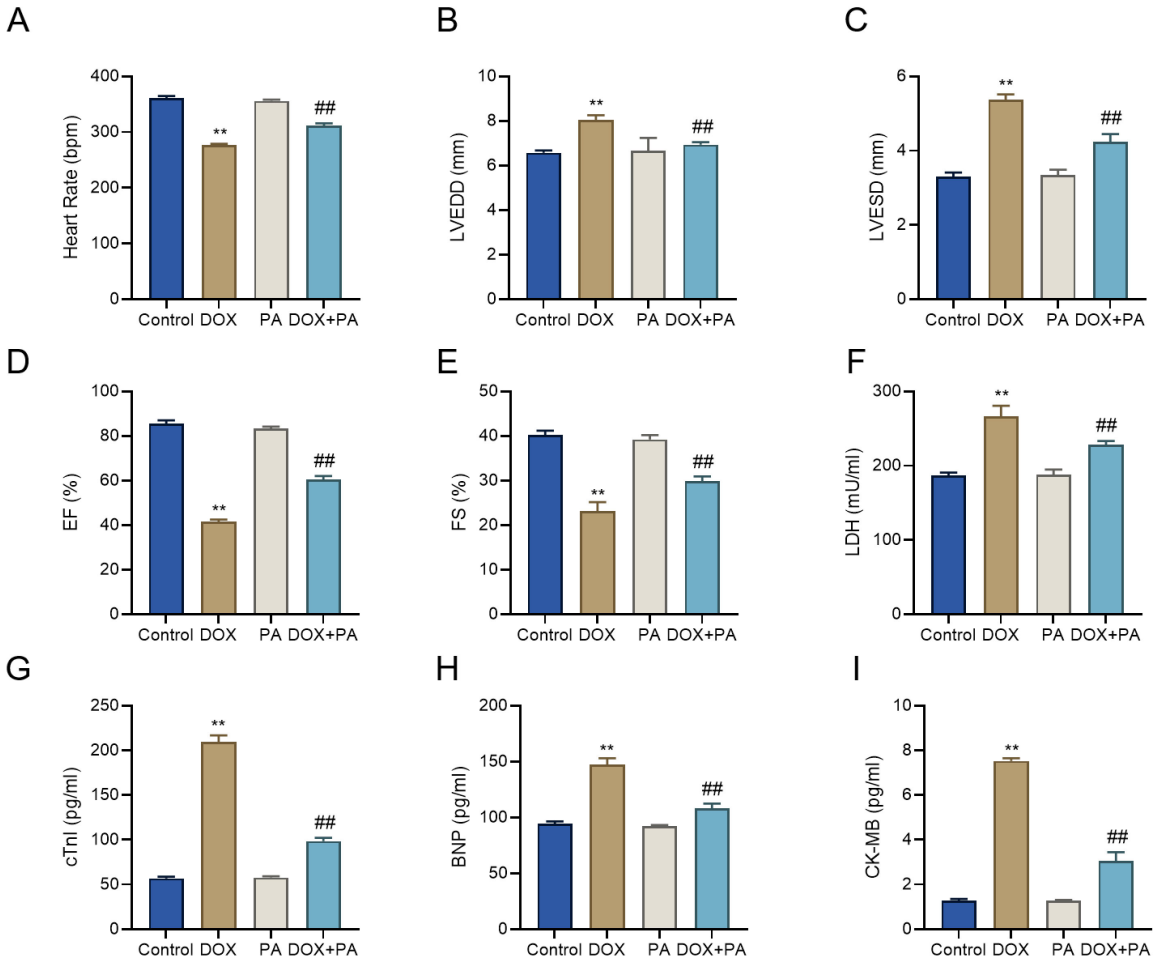

Fig. 6. PA improves cardiac performance in DOX-treated rats. (A) Heart rate. (B) Left ventricular end-diastolic dimension (LVEDD). (C) Left ventricular end-systolic dimension (LVESD). (D) Ejection fraction (EF). (E) Fractional shortening (FS). (F) Serum lactate dehydrogenase (LDH). (G) Cardiac troponin I (cTnI). (H) Brain natriuretic peptide (BNP). (I) Creatine kinase-MB (CK-MB). Data are presented as mean ± SD (n = 3 independent experiments for *in vitro* assays; n = 9 animals per group for *in vivo* studies). $^{**}p < 0.01$ vs. control; $^{\#\#}p < 0.01$ vs. DOX.

tory cytokines (TNF-α, IL-6, IL-1β) and restored redox balance by decreasing MDA and increasing GSH and SOD levels ($p < 0.01$; Fig. 8A–F).

These findings highlight that PA confers cardioprotection against DOX-induced injury by simultaneously suppressing inflammation and oxidative stress.

Discussion

The present study provides compelling evidence that PA effectively attenuates DOX-induced cardiac injury by simultaneously alleviating apoptosis, oxidative imbalance, inflammatory response, and DNA damage in cardiomyocytes. As DOX-induced cardiotoxicity remains a significant clinical challenge limiting its therapeutic application in cancer treatment, our findings hold substantial translational relevance by highlighting PA as a promising cardioprotective agent.

A previous study has established oxidative imbalance and programmed cell death as key mechanisms underlying DOX-mediated cardiomyocyte damage [8]. Consistent with this findings, we observed significant increases in oxidative stress markers (ROS, MDA) and apoptosis-related proteins (cleaved-caspase-3, Bax/Bcl-2 ratio, cleaved-PARP) following DOX treatment. Notably, PA pretreatment significantly reversed these pathological alterations by suppressing ROS production, enhancing antioxidant enzyme activity (SOD, GSH), and modulating apoptotic protein expression. Mechanistically, PA appears to inhibit mitochondrial-dependent apoptosis by preventing cytochrome c release, thus blocking subsequent caspase activation and apoptosome formation, consistent with previous reports of mitochondrial protection in oxidative stress-induced apoptosis [27,28].

Our findings further highlight the novel role of PA in mitigating DOX-induced genotoxicity. PA signifi-

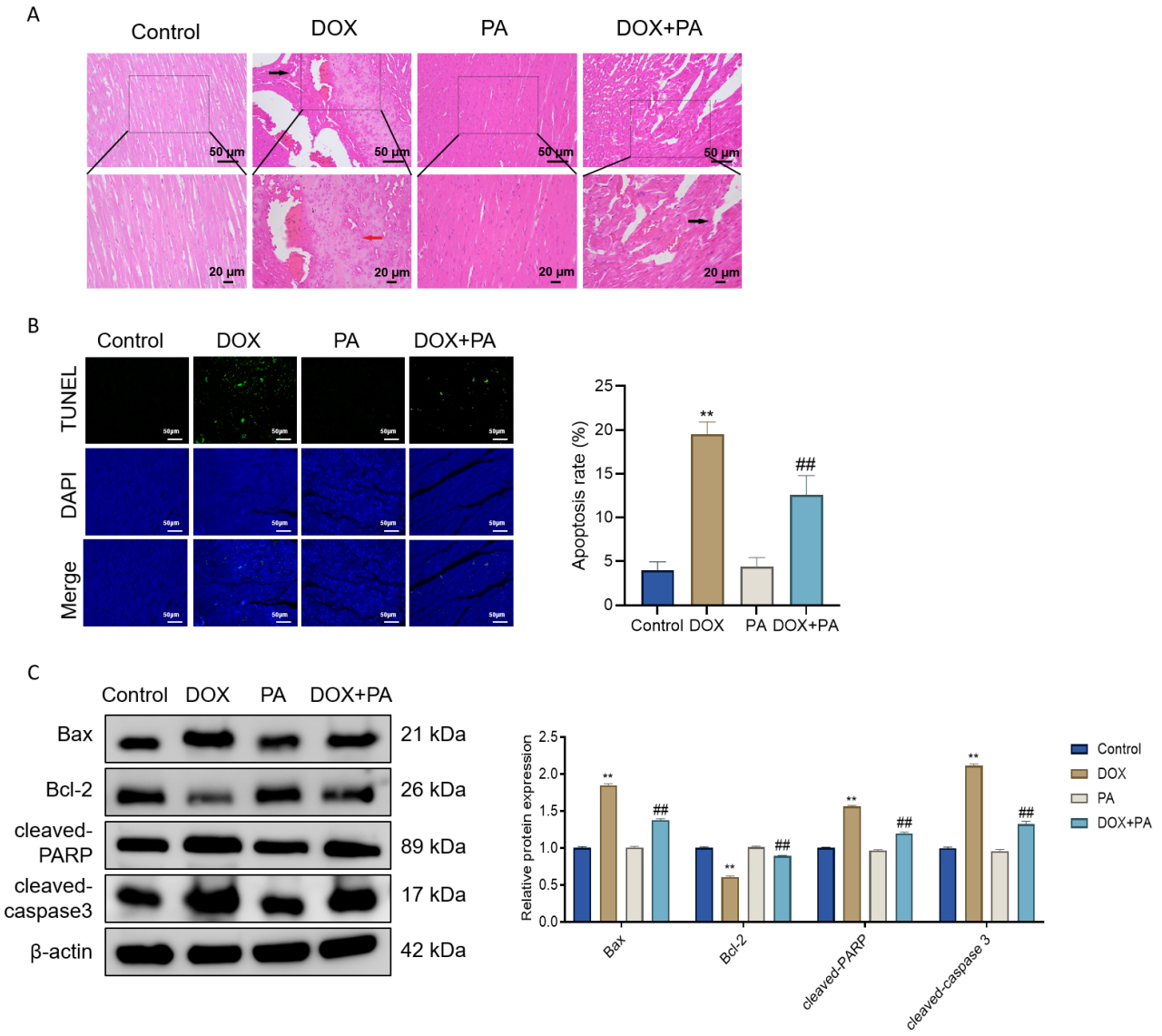

Fig. 7. PA mitigates DOX-induced myocardial apoptosis and structural injury *in vivo*. (A) Hematoxylin and Eosin (HE) staining of cardiac tissues in the control, DOX, PA, and DOX + PA groups. Red arrow indicates myocardial fiber breakage and necrosis; black arrows indicate inflammatory cell infiltration. (B) TUNEL staining of apoptotic cells (green) with DAPI-stained nuclei (blue). (C) Western blot analysis of Bax, Bcl-2, cleaved-PARP, and cleaved-caspase 3. Data are presented as mean ± SD (n = 3 independent experiments for *in vitro* assays; n = 9 animals per group for *in vivo* studies). $^{**}p < 0.01$ vs. control; $^{\#\#}p < 0.01$ vs. DOX.

cantly reduced DOX-induced DNA damage by suppressing γH2AX and p-ATR activation, thereby inhibiting downstream p53/p21 signaling. This regulatory effect may limit excessive cell cycle arrest and secondary apoptotic signaling, reinforcing the role of PA in genomic stability under oxidative stress [29–31]. Such multi-targeted molecular interventions underscore the advantages of PA compared to previously reported single-pathway agents such as quercetin and resveratrol [32–34].

Notably, the cardioprotective effects of PA gain broader significance when contextualized with its established anticancer properties. Recent studies demonstrated that PA exerts tumor-suppressive effects through diverse mechanisms: reversing P-glycoprotein-mediated multidrug resistance [35], inducing ROS-dependent apoptosis via c-Jun N-terminal kinase/Endoplasmic Reticulum (JNK/ER) stress activation in lung cancer [36], regulating Bcl-2/IAP family proteins in bladder cancer [37], and inhibiting NF-κB-driven metastasis in breast cancer [38]. This pleiotropic activity profile suggests PA may synergize with doxorubicin chemotherapy by simultaneously protecting cardiomyocytes (this study) and enhancing tumor sensitivity [35]. The cardioprotective dose identified in the present study (10 mg/kg *in vivo*) is consistent with antitumor-effective doses reported in xenograft models [36], supporting its therapeutic potential. Future studies should explore

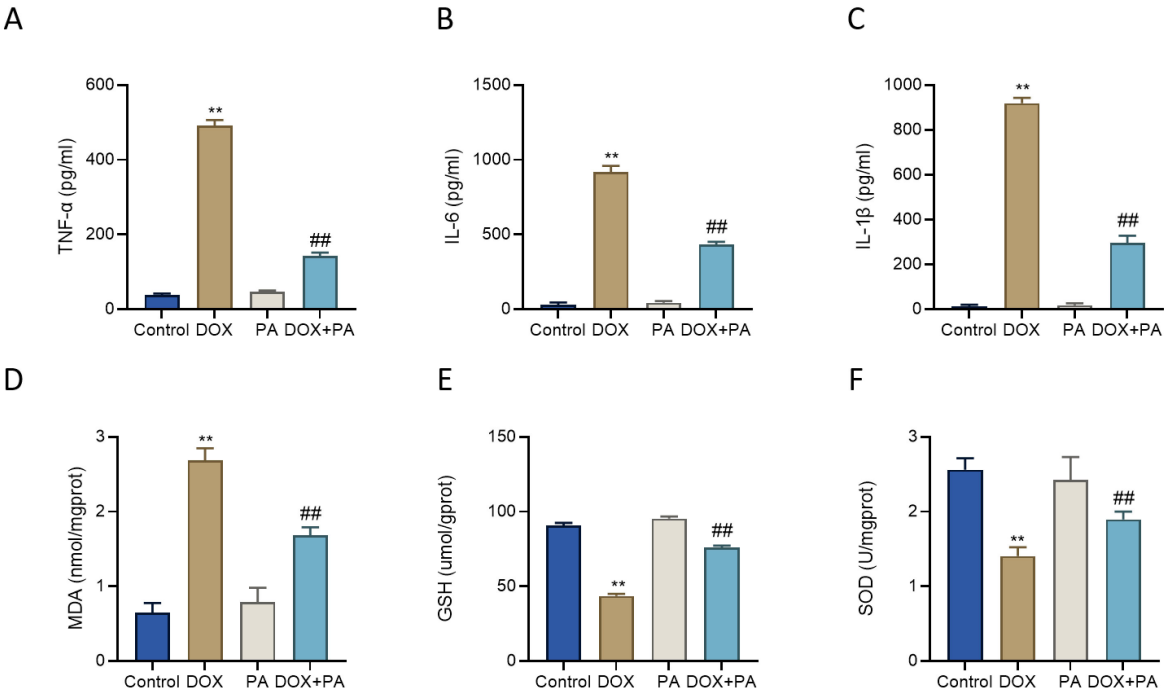

Fig. 8. PA reduces DOX-induced inflammation and oxidative imbalance in rats. (A) Serum TNF-α. (B) Serum IL-6. (C) Serum IL-1β. (D) Malondialdehyde (MDA). (E) Glutathione (GSH). (F) Superoxide dismutase (SOD) activity. Data are presented as mean $\pm$ SD (n = 9 animals per group for *in vivo* studies). $^{**}p < 0.01$ vs. control; $^{\#\#}p < 0.01$ vs. DOX.

this combinatorial strategy while addressing translational considerations such as formulation development, pharmacokinetics, and long-term safety profiling.

Moreover, PA demonstrated substantial anti-inflammatory effects, as evidenced by reductions in proinflammatory mediators including TNF-α, IL-6, and IL-1β. This observation complements previous evidence highlighting the anti-inflammatory and antioxidant properties of PA across diverse pathological contexts [39–42]. Notably, our study expands the pharmacological relevance of PA by elucidating its role in mitigating chemotherapy-associated cardiotoxicity through a unique multi-pathway mechanism, simultaneously targeting oxidative stress, DNA damage, inflammation, and apoptosis. These integrative effects distinguish PA from single-pathway agents and underscore its potential as a combinatorial therapeutic strategy.

Consistent with our cellular results, *in vivo* rat experiments further demonstrated that PA reduced serum cardiac injury biomarkers (LDH, cTnI, BNP, CK-MB). The sequential treatment design intentionally mirrors real-world clinical practice, where cardio-protective agents are typically initiated after detection of cardiac injury markers rather than prophylactically. The significant reduction in cardiac injury biomarkers (LDH, cTnI) and histopathological damage despite post-DOX PA administration underscores its therapeutic, not solely preventive, potential. Histological analyses provided further support, revealing myocardial fiber disruption, cellular necrosis, and inflammatory infiltration in DOX-treated rats, consistent with previous animal studies on anthracycline-induced cardiotoxicity [43,44]. Notably, these pathological alterations were markedly attenuated following PA administration, suggesting strong anti-necrotic and anti-inflammatory effects at the tissue level, paralleling protective actions reported for other phytochemicals in animal models [24,45]. Furthermore, PA effectively reduced cardiomyocyte apoptosis, suppressed inflammatory cytokines, decreased oxidative stress markers, and restored antioxidant enzyme activities, consistent with our *in vitro* findings. Collectively, these findings underscore the promise of PA as a viable cardioprotective candidate, warranting further investigation in preclinical and clinical settings.

A key innovation of this study lies in elucidating the comprehensive protective mechanisms of PA against DOX-induced cardiotoxicity. Whereas previous investigations primarily emphasized single mechanisms, our results demonstrate a multi-targeted approach, simultaneous inhibition of apoptosis, oxidative stress, inflammation, and DNA damage. These findings support further exploration of PA as a foundation for developing integrative cardioprotective therapies, potentially in synergy with existing pharmacological or lifestyle interventions.

Despite these significant findings, several limitations warrant further consideration. First, the study primarily employed an acute cardiotoxicity model induced by short-term

DOX exposure in rats. Future investigations should evaluate the efficacy of PA in chronic cardiotoxicity models that better reflect long-term chemotherapy regimens and clinical scenarios. Second, while multiple pathways were examined, additional studies using pathway-specific inhibitors, agonists, or genetic manipulation are required to precisely define the molecular targets of PA. Moreover, investigating potential synergistic effects between PA and established cardioprotective agents, particularly through pathways such as Nrf2/ARE or P53 signaling [46], could further enhance therapeutic efficacy. Third, while H9c2 cells represent a valuable screening tool, their embryonic origin may not fully mimic adult cardiomyocyte physiology, emphasizing the need for validation in primary cardiomyocytes or human induced pluripotent stem cell (iPSC)-derived cardiomyocytes. Furthermore, although the selected PA dosage demonstrated efficacy without observable toxicity, comprehensive safety assessments, including hepatic and kidney function assessments and long-term toxicity profiling, remain essential for clinical translation. Collectively, these considerations highlight important directions for future research to advance PA toward therapeutic application. Ultimately, integrating PA into personalized therapeutic regimens with routine cardiac function monitoring may significantly improve clinical outcomes and patient well-being during chemotherapy.

In conclusion, this study provides the first evidence that PA significantly mitigates DOX-induced cardiac dysfunction through comprehensive modulation of apoptosis, oxidative imbalance, inflammatory responses, and DNA damage. These multi-targeted protective effects establish PA as a promising cardioprotective compound, paving the way for clinical translation and providing a foundation for the development of innovative strategies to mitigate chemotherapy-associated cardiotoxicity.

Conclusion

This study revealed that PA significantly alleviated DOX-associated cardiac injury by simultaneously inhibiting oxidative imbalance, inflammatory responses, apoptosis, and DNA damage in cellular and animal models. These findings underscore its potential as a promising therapeutic strategy to prevent chemotherapy-related cardiac injury. However, further mechanistic research and clinical evaluation are warranted to facilitate its translation into clinical practice.

Availability of Data and Materials

The datasets used and/or analyzed during the current study are available from the corresponding author on reasonable request.

Author Contributions

YS and DW contributed to the study conception, design, data acquisition, analysis, interpretation, drafting of the manuscript and critical revision of the manuscript. Both authors read and approved the final manuscript. Both authors have participated sufficiently in the work and agreed to be accountable for all aspects of the work.

Ethics Approval and Consent to Participate

All animal procedures were approved by the Experimental Animal Ethics Committee of the Guangdong Medical Experimental Animal Center (approval number: D202507-22), affiliated with the Guangdong Health Commission.

Acknowledgment

Not applicable.

Funding

This research received no external funding.

Conflict of Interest

The authors declare no conflict of interest.

References

[1] Zhao H, Yu J, Zhang R, Chen P, Jiang H, Yu W. Doxorubicin prodrug-based nanomedicines for the treatment of cancer. European Journal of Medicinal Chemistry. 2023; 258: 115612. https://doi.org/10.1016/j.ejmech.2023.115612.

[2] Kciuk M, Gielecińska A, Mujwar S, Kołat D, Kałuzińska-Kołat Ż, Celik I, *et al*. Doxorubicin-An Agent with Multiple Mechanisms of Anticancer Activity. Cells. 2023; 12: 659. https://doi.org/10.3390/cells12040659.

[3] Kalafatovic D, Nobis M, Son J, Anderson KI, Ulijn RV. MMP-9 triggered self-assembly of doxorubicin nanofiber depots halts tumor growth. Biomaterials. 2016; 98: 192–202. https://doi.org/10.1016/j.biomaterials.2016.04.039.

[4] Christidi E, Brunham LR. Regulated cell death pathways in doxorubicin-induced cardiotoxicity. Cell Death & Disease. 2021; 12: 339. https://doi.org/10.1038/s41419-021-03614-x.

[5] Zamorano JL, Lancellotti P, Muñoz DR, Aboyans V, Asteggiano R, Galderisi M, *et al*. 2016 ESC Position Paper on cancer treatments and cardiovascular toxicity developed under the auspices of the ESC Committee for Practice Guidelines. Kardiologia Polska. 2016; 74: 1193–1233. https://doi.org/10.5603/KP.2016.0156. (In Polish)

[6] Cardinale D, Colombo A, Bacchiani G, Tedeschi I, Meroni CA, Veglia F, *et al*. Early detection of anthracycline cardiotoxicity and improvement with heart failure therapy. Circulation. 2015; 131: 1981–1988. https://doi.org/10.1161/CIRCULATIONAHA.114.013777.

[7] Khan AA, Ashraf A, Singh R, Rahim A, Rostom W, Hussain M, *et al*. Incidence, time of occurrence and response to heart failure therapy in patients with anthracycline cardiotoxicity. Internal Medicine Journal. 2017; 47: 104–109. https://doi.org/10.1111/imj.13305.

[8] Kong CY, Guo Z, Song P, Zhang X, Yuan YP, Teng T, *et al*. Underlying the Mechanisms of Doxorubicin-Induced Acute Cardiotoxicity: Oxidative Stress and Cell Death. International Journal of Biological Sciences. 2022; 18: 760–770. https://doi.org/10.7150/ijbs.65258.

[9] Wu BB, Leung KT, Poon ENY. Mitochondrial-Targeted Therapy for Doxorubicin-Induced Cardiotoxicity. International Journal of Molecular Sciences. 2022; 23: 1912. https://doi.org/10.3390/ijms23031912.

[10] Mf NM, Arunachalam S, Sheikh A, Saraswathiamma D, Albawardi A, Al Marzooqi S, *et al*. α-Bisabolol: A Dietary Sesquiterpene that Attenuates Apoptotic and Nonapoptotic Cell Death Pathways by Regulating the Mitochondrial Biogenesis and Endoplasmic Reticulum Stress-Hippo Signaling Axis in Doxorubicin-Induced Acute Cardiotoxicity in Rats. ACS Pharmacology & Translational Science. 2024; 7: 2694–2705. https://doi.org/10.1021/acsptsci.4c00108.

[11] Vitale R, Marzocco S, Popolo A. Role of Oxidative Stress and Inflammation in Doxorubicin-Induced Cardiotoxicity: A Brief Account. International Journal of Molecular Sciences. 2024; 25: 7477. https://doi.org/10.3390/ijms25137477.

[12] Wu Y, Ying J, Zhu X, Xu C, Wu L. Pachymic acid suppresses the inflammatory response of chondrocytes and alleviates the progression of osteoarthritis via regulating the Sirtuin 6/NF-κB signal axis. International Immunopharmacology. 2023; 124: 110854. https://doi.org/10.1016/j.intimp.2023.110854.

[13] Wen H, Wu Z, Hu H, Wu Y, Yang G, Lu J, *et al*. The antitumor effect of pachymic acid on osteosarcoma cells by inducing PTEN and Caspase 3/7-dependent apoptosis. Journal of Natural Medicines. 2018; 72: 57–63. https://doi.org/10.1007/s11418-017-1117-2.

[14] Yang T, Tian S, Wang Y, Ji J, Zhao J. Antitumor activity of pachymic acid in cervical cancer through inducing endoplasmic reticulum stress, mitochondrial dysfunction, and activating the AMPK pathway. Environmental Toxicology. 2022; 37: 2121–2132. https://doi.org/10.1002/tox.23555.

[15] Wang S, Tan W, Zhang L, Jiang H. Pachymic Acid Protects Against Bleomycin-Induced Pulmonary Fibrosis by Suppressing Fibrotic, Inflammatory, and Oxidative Stress Pathways in Mice. Applied Biochemistry and Biotechnology. 2024; 196: 3344–3355. https://doi.org/10.1007/s12010-023-04686-5.

[16] Lu C, Cai D, Ma J. Pachymic Acid Sensitizes Gastric Cancer Cells to Radiation Therapy by Upregulating Bax through Hypoxia. The American Journal of Chinese Medicine. 2018; 46: 875–890. https://doi.org/10.1142/S0192415X18500465.

[17] Liu Z, Zhou W, Liu Q, Huan Z, Wang Q, Ge X. Pachymic Acid Prevents Hemorrhagic Shock-Induced Cardiac Injury by Suppressing M1 Macrophage Polarization and NF-[Formula: see text]B Signaling Pathway. The American Journal of Chinese Medicine. 2023; 51: 2157–2173. https://doi.org/10.1142/S0192415X23500921.

[18] Liu D, Ding J, Li Z, Lu Y. Pachymic acid (PA) inhibits ferroptosis of cardiomyocytes via activation of the AMPK in mice with ischemia/reperfusion-induced myocardial injury. Cell Biology International. 2024; 48: 46–59. https://doi.org/10.1002/cbin.12090.

[19] Wang S, Wang L, Cheng H, Li H, Zhang Q, He C, *et al*. Targeting autophagy in doxorubicin-induced cardiotoxicity: A comprehensive review of scientific landscapes and therapeutic innovations. Ageing Research Reviews. 2025; 110: 102818. https://doi.org/10.1016/j.arr.2025.102818.

[20] Kimes BW, Brandt BL. Properties of a clonal muscle cell line from rat heart. Experimental Cell Research. 1976; 98: 367–381. https://doi.org/10.1016/0014-4827(76)90447-x.

[21] Liehr T, Kankel S, Hardt KS, Buhl EM, Noels H, Keller DT, *et al*. Genetic and Molecular Characterization of H9c2 Rat Myoblast Cell Line. Cells. 2025; 14: 502. https://doi.org/10.3390/cells14070502.

[22] Zhao L, Qi Y, Xu L, Tao X, Han X, Yin L, *et al*. MicroRNA-140-5p aggravates doxorubicin-induced cardiotoxicity by promoting myocardial oxidative stress via targeting Nrf2 and Sirt2. Redox Biology. 2018; 15: 284–296. https://doi.org/10.1016/j.redox.2017.12.013.

[23] Guo R, Wu K, Chen J, Mo L, Hua X, Zheng D, *et al*. Exogenous hydrogen sulfide protects against doxorubicin-induced inflammation and cytotoxicity by inhibiting p38MAPK/NFκB pathway in H9c2 cardiac cells. Cellular Physiology and Biochemistry. 2013; 32: 1668–1680. https://doi.org/10.1159/000356602.

[24] Abdulkareem Aljumaily SA, Demir M, Elbe H, Yigitturk G, Bicer Y, Altinoz E. Antioxidant, anti-inflammatory, and anti-apoptotic effects of crocin against doxorubicin-induced myocardial toxicity in rats. Environmental Science and Pollution Research International. 2021; 28: 65802–65813. https://doi.org/10.1007/s11356-021-15409-w.

[25] Younis NN, Salama A, Shaheen MA, Eissa RG. Pachymic Acid Attenuated Doxorubicin-Induced Heart Failure by Suppressing miR-24 and Preserving Cardiac Junctophilin-2 in Rats. International Journal of Molecular Sciences. 2021; 22: 10710. https://doi.org/10.3390/ijms221910710.

[26] Li K, Sung RYT, Huang WZ, Yang M, Pong NH, Lee SM, *et al*. Thrombopoietin protects against in vitro and in vivo cardiotoxicity induced by doxorubicin. Circulation. 2006; 113: 2211–2220. https://doi.org/10.1161/CIRCULATIONAHA.105.560250.

[27] Rawat PS, Jaiswal A, Khurana A, Bhatti JS, Navik U. Doxorubicin-induced cardiotoxicity: An update on the molecular mechanism and novel therapeutic strategies for effective management. Biomedicine & Pharmacotherapy. 2021; 139: 111708. https://doi.org/10.1016/j.biopha.2021.111708.

[28] Santucci R, Sinibaldi F, Cozza P, Polticelli F, Fiorucci L. Cytochrome c: An extreme multifunctional protein with a key role in cell fate. International Journal of Biological Macromolecules. 2019; 136: 1237–1246. https://doi.org/10.1016/j.ijbiomac.2019.06.180.

[29] Kopp B, Khoury L, Audebert M. Validation of the γH2AX biomarker for genotoxicity assessment: a review. Archives of Toxicology. 2019; 93: 2103–2114. https://doi.org/10.1007/s00204-019-02511-9.

[30] McSweeney KM, Bozza WP, Alterovitz WL, Zhang B. Transcriptomic profiling reveals p53 as a key regulator of doxorubicin-induced cardiotoxicity. Cell Death Discovery. 2019; 5: 102. https://doi.org/10.1038/s41420-019-0182-6.

[31] He Y, Wang Z, Hu Y, Yi X, Wu L, Cao Z, *et al*. Sensitive and selective monitoring of the DNA damage-induced intracellular p21 protein and unraveling the role of the p21 protein in DNA repair and cell apoptosis by surface plasmon resonance. The Analyst. 2020; 145: 3697–3704. https://doi.org/10.1039/c9an02464f.

[32] Dorostkar H, Haghiralsadat BF, Hemati M, Safari F, Hassanpour A, Naghib SM, *et al*. Reduction of Doxorubicin-Induced Cardiotoxicity by Co-Administration of Smart Liposomal Doxorubicin and Free Quercetin: In Vitro and In Vivo Studies. Pharmaceutics. 2023; 15: 1920. https://doi.org/10.3390/pharmaceutics15071920.

[33] Dulf PL, Coadă CA, Florea A, Moldovan R, Baldea I, Dulf DV, *et al*. Mitigating Doxorubicin-Induced Cardiotoxicity through Quercetin Intervention: An Experimental Study in Rats. Antioxidants. 2024; 13: 1068. https://doi.org/10.3390/antiox13091068.

[34] Dong Q, Chen L, Lu Q, Sharma S, Li L, Morimoto S, *et al*. Quercetin attenuates doxorubicin cardiotoxicity by modulating Bmi-1 expression. British Journal of Pharmacology. 2014; 171: 4440–4454. https://doi.org/10.1111/bph.12795.

[35] Li Y, Li X, Lu Y, Chaurasiya B, Mi G, Shi D, *et al*. Co-delivery of Poria cocos extract and doxorubicin as an 'all-in-one' nanocarrier to combat breast cancer multidrug resistance during chemotherapy. Nanomedicine: Nanotechnology, Biology, and Medicine. 2020; 23: 102095. https://doi.org/10.1016/j.nano.2019.102095.

[36] Ma J, Liu J, Lu C, Cai D. Pachymic acid induces apoptosis via activating ROS-dependent JNK and ER stress pathways in lung cancer cells. Cancer Cell International. 2015; 15: 78. https://doi.org/10.1186/s12935-015-0230-0.

[37] Jeong JW, Lee WS, Go SI, Nagappan A, Baek JY, Lee JD, *et al*. Pachymic Acid Induces Apoptosis of EJ Bladder Cancer Cells by DR5 Up-Regulation, ROS Generation, Modulation of Bcl-2 and IAP Family Members. Phytotherapy Research. 2015; 29: 1516–1524. https://doi.org/10.1002/ptr.5402.

[38] Ling H, Zhang Y, Ng KY, Chew EH. Pachymic acid impairs breast cancer cell invasion by suppressing nuclear factor-κB-dependent matrix metalloproteinase-9 expression. Breast Cancer Research and Treatment. 2011; 126: 609–620. https://doi.org/10.1007/s10549-010-0929-5.

[39] Gui Y, Sun L, Liu R, Luo J. Pachymic acid inhibits inflammation and cell apoptosis in lipopolysaccharide (LPS)-induced rat model with pneumonia by regulating NF-κB and MAPK pathways. Allergologia et Immunopathologia. 2021; 49: 87–93. https://doi.org/10.15586/aei.v49i5.468.

[40] Jiang F, Zhu T, Yang C, Chen Y, Fu Z, Jiang L, *et al*. Pachymic Acid Inhibits Growth and Metastatic Potential in Liver Cancer HepG2 and Huh7 Cells. Biological & Pharmaceutical Bulletin. 2023; 46: 35–41. https://doi.org/10.1248/bpb.b22-00440.

[41] Jiang Y, Fan L. Evaluation of anticancer activities of Poria cocos ethanol extract in breast cancer: In vivo and in vitro, identification and mechanism. Journal of Ethnopharmacology. 2020; 257: 112851. https://doi.org/10.1016/j.jep.2020.112851.

[42] Miao G, Han J, Zhang J, Wu Y, Tong G. Targeting Pyruvate Kinase M2 and Hexokinase II, Pachymic Acid Impairs Glucose Metabolism and Induces Mitochondrial Apoptosis. Biological & Pharmaceutical Bulletin. 2019; 42: 123–129. https://doi.org/10.1248/bpb.b18-00730.

[43] Ling G, Ge F, Li W, Wei Y, Guo S, Zhang Y, *et al*. Anthracycline-induced cardiotoxicity: emerging mechanisms and therapies. Medicine Plus. 2025; 2: 100074. https://doi.org/10.1016/j.medp.2025.100074.

[44] Xie S, Sun Y, Zhao X, Xiao Y, Zhou F, Lin L, *et al*. An update of the molecular mechanisms underlying anthracycline induced cardiotoxicity. Frontiers in Pharmacology. 2024; 15: 1406247. https://doi.org/10.3389/fphar.2024.1406247.

[45] Birdal O, Ferah Okkay I, Okkay U, Bayram C, Mokthare B, Ertugrul MS, *et al*. Protective effects of arbutin against doxorubicin-induced cardiac damage. Molecular Biology Reports. 2024; 51: 532. https://doi.org/10.1007/s11033-024-09488-4.

[46] Ibrahim SG, Abu-Dief AM, Gad AM, Gad ES, Alzahrani AYA, Alraih AM, *et al*. Methylene Blue Mitigates Doxorubicin-Induced Cardiotoxicity via KEAP1/NRF2/GPX-4/Caspase3 Modulation. International Journal of Molecular Sciences. 2025; 26: 7680. https://doi.org/10.3390/ijms26167680.